DOI: 10.1070/RCR4818

Magnetic isotopes as a means to elucidate Earth and environmental chemistry

Anatoly L. Buchachenko

N.N.Semenov Institute of Chemical Physics, Russian Academy of Sciences
ul. Kosygina 4, 119991 Moscow, Russian Federation
Institute of Problems of Chemical Physics, Russian Academy of Sciences
prosp. Academika Semenova 1, 142432 Chernogolovka, Moscow Region, Russian Federation
Science Center in Chernogolovka of the Russian Academy of Sciences
ul. Lesnaya 9, 142432 Chernogolovka, Moscow Region, Russian Federation
P.G.Demidov Yaroslavl State University
ul. Sovetskaya 14, 150003 Yaroslavl, Russian Federation
Department of Chemistry, Lomonosov Moscow State University
Leninskie Gory 1, stroenie 3, 119991 Moscow, Russian Federation

In Earth and environmental chemistry, magnetic isotopes provide a universal means to identify reaction mechanisms. Mass-independent fractionation of isotopes as a signature of a mechanism occurs by two ways: first, *via* the magnetic isotope effect (MIE), which is controlled by magnetic, or hyperfine, coupling between unpaired electrons and magnetic nuclei in paramagnetic species (particularly, in radicals), and, second, *via* the nuclear volume effect (NVE), which is induced by the volume difference between isotopic nuclei. The MIE is the dependence of the reaction rates on the nuclear magnetic moment of reactants and fractionates magnetic and nonmagnetic isotopes, whereas NVE fractionates isotopes with different nuclear volumes. Both effects, MIE and NVE, are supposed to coexist in condensed phases. A decisive test for their differentiation is illustrated by the example of radical pairs with mercury nuclei. Namely, if isotope fractionation is controlled by MIE, the ratio $\Delta^{201}Hg/\Delta^{199}Hg$ is expected to be in the range of 1.05 – 1.25 for isotopic enrichment and 0.80 – 0.92 for depletion. If isotope fractionation is controlled by NVE, this ratio is estimated to be in the range of 0.50 – 0.62. In contrast to MIE-induced bidirectional fractionation controlled by the direction of coherent spin conversion of the radical pair (triplet – singlet or *vice versa*), the NVE induces unidirectional, universal isotope fractionation, which is almost independent of the reaction mechanism. In contrast to MIE which exhibits inversion of the fractionation sign depending on the spin multiplicity of reactants, NVE is incompatible with the inversion of the fractionation sign. The MIE is an unambiguous indicator of the radical mechanisms and dominates in chemical reactions, whereas NVE prevails in nonchemical processes. Chemical scenarios of MIE-induced oxygen, sulfur, iron, silicon, tin, mercury, germanium and uranium isotope fractionation in photostimulated and dark reactions are analyzed in terms of reaction mechanisms including reactions in living organisms. In conclusion, some restrictions, uncertainties and problems in Earth and environmental chemistry are discussed.
The bibliography includes 92 references.

Contents

1. Introduction 728
2. Mass-independent isotope fractionation 728
3. Oxygen isotopes 729
4. Magnetic isotopes of sulfur 730
5. Iron isotopes 732
6. Tin and germanium isotopes 732
7. Magnetic isotopes of silicon 733
8. Uranium isotopes 734
9. Mercury isotopes 734
10. A test: MIE or NVE? 735
11. Chemical scenarios of MIE-induced mercury isotope fractionation 736
12. Isotope fractionation in nonchemical processes 737
13. Magnetic isotopes of mercury in living organisms 737
14. Conclusion: achievements and problems 739

© 2018 Uspekhi Khimii, Russian Academy of Sciences and Turpion Ltd.

1. Introduction

Magnetic nuclei are specific: they create internal, local magnetic fields on the unpaired electrons of chemically reactive paramagnetic species. The energy of electron–nuclear magnetic interaction also known as hyperfine coupling or Fermi interaction is negligible and may be certainly ignored in the total balance of chemical energy. However, besides energy there is yet another, much more strict and powerful controlling factor, *viz*., the angular momentum. The conservation of angular momentum (electron spin) is a fundamental and universal principle, namely, all chemical reactions are spin-selective, they are allowed only for those spin states of reactants whose total spin is identical to that of products. Contributing next to nothing in chemical energy, magnetic interactions are the only ones that are able to change the electron spin of reactants and switch over the reaction between spin-forbidden and spin-allowed channels.

The reactivity difference between species with magnetic and nonmagnetic nuclei is the mass-independent isotope effect. Since these nuclei differ in the number of neutrons, the mass-independent isotope effect is composed of two components, the magnetic isotope effect (MIE) and he nuclear volume effect (NVE); both will be analyzed in this paper.

The MIE was predicted in 1971[1] and for the first time detected experimentally in 1976.[2,3] It was christened as the MIE because it is controlled by hyperfine coupling; it results in the dependence of the reaction rates on the nuclear magnetic moments of reactants and fractionates isotopes by their magnetic moments rather than masses. Due to this property it provides a new powerful technology of isotope fractionation and a new tool for mechanistic chemistry, geo- and biochemistry and space chemistry; it allows tracing the chemical evolution of Matter, the genesis and chemical history of substances in Nature.[4–6] The observation of MIE is an unambiguous and the most reliable indication of the radical mechanism of a reaction, it implies generation of a radical pair as a two-spin system by dissociation of molecules or by electron transfer. The pair can exist in two spin states, a singlet (total electron spin is zero) or a triplet one (total electron spin is unity). Being chemically identical, these states differ in reactivity; magnetic interactions produce spin conversion of the pair, switching over the reaction between spin-forbidden and spin-allowed channels, controlling the reaction rates.[7] The MIE is shown to function in a great variety of processes in physics and chemistry,[8,9] in biology and medicine.[10] It is remarkable that the MIE magnitude is usually ten times larger than that of classical, mass-dependent isotope effect. As we will see later, in some biochemical reactions the MIE reaches even 200%–300%.

A.L.Buchachenko. Professor of the Institute of Chemical Physics; Professor of the Moscow State University; the Member of the Russian Academy of Sciences.
Telephone: +7 (495)939–7128,
e-mail: alb9397128@yandex.ru; abuchach@chph.ras.ru
Current research interests: physics of chemical reactions, magnetic isotopy, magneto-biology, isotope effects, molecular ferromagnets.

Received 5 March 2017

Bigeleisen[11] was the first who advanced the idea that not only the nuclear mass, but also the nuclear volume (more exactly, the radius) may appear to be significant in the fractionation of heavy elements. Unlike the mass-dependent isotope effect originating from the vibrational energy difference between isotopic molecules, NVE is due to the energy difference between valence electrons. It is reliably detected mostly for heavy elements, for which relativistic effects are important.[12] Bigeleisen [13,14] developed a theory of the effect and suggested a method to calculate the isotope separation factor from the parameters of molecular spectra of isotopomers. The NVE was detected reliably in the atomic spectra as shifts of spectral lines; the contribution of the NVE to fractionation of isotopes seems to depend on the type of the chemical process and will be discussed below (see Sections 10 and 12).

There are two aspects in isotopic Earth and environmental chemistry: first, isotope effects produce isotope fractionation as a memory of the birth and transformation of molecules; second, isotopes function as labels tracing the exchange between the atmosphere–continent–ocean interfaces, certifying the fate of chemical events.[15,16] This paper focuses on the first, the most important function, *i.e*., fractionation of isotopes as itself. Its goal is to critically summarize experimental findings and theoretical ideas, to identify and discuss chemical reactions responsible for isotope fractionation, to formulate mechanisms of the isotope-sorting reactions in order to foresee and control these reactions and their hazards to the environment and living organisms and, at last, to emphasize some restrictions, uncertainties and problems in this highly important field of chemistry.

2. Mass-independent isotope fractionation

By definition, mass-independent isotope effects are those creating an anomalous isotopic distribution incompatible with that expected from the mass-dependent isotope effect. For a particular case of the oxygen isotope triad, in terms of the delta notation the mass-independent isotope effect is traditionally expressed as a scaled deviation:

$$\Delta^{17}O \approx \delta^{17}O - 0.5\,\delta^{18}O \qquad (1)$$

where

$$\delta^{17}O = ({}^{17}R_x/{}^{17}R_{st} - 1) \times 10^3$$

$$\delta^{18}O = ({}^{18}R_x/{}^{18}R_{st} - 1) \times 10^3$$

Here ${}^{17}R_x = ({}^{17}O/{}^{16}O)$ is the fraction of ^{17}O in the analyzed material, ${}^{17}R_{st}$ is that in a certain standard, ${}^{18}R_x = ({}^{18}O/{}^{16}O)$ is the fraction of ^{18}O in the analyzed material and ${}^{18}R_{st}$ is that in the standard. All magnitudes are usually expressed in per mille (0.1%). Equations similar to Eqn (1) are used for other isotopic families; as will be discussed in Sections 9 and 14, these equations are approximate and should be used with care.

Hulsten and Thode[17] were the first who observed a noticeable deviation of sulfur isotope contents in iron meteorites from that which might be expected from the mass-dependent effect. More recently, Clayton *et al*.[18,19] detected a similar deviation for oxygen in calcium–aluminium inclusions from carbonaceous chondrite Allende; they found $\delta^{17}O = \delta^{18}O$ in contrast to the expected $\delta^{17}O \approx 0.5\,\delta^{18}O$. These anomalies were ascribed to the *non-*

chemical events (invasion of extraterrestrial material). However, in 1983 Thiemens and Heidenreich [20] discovered that the formation of ozone from molecular oxygen does not conform to the mass-dependent isotope effect; they ingeniously identified it as a *chemically induced* mass-independent isotope effect. It also successfully explained isotopic anomalies in meteorites; the results are summarized in exhaustive reviews by Thiemens [21, 22] and Weston.[23, 24]

The effect operates predominantly in the gas-phase reactions (atmospheric and space chemistry). In particular, reactions of this type produce surprisingly large anomalous enrichments in ^{17}O of stratospheric CO_2 that vary systematically with latitude, altitude, and season.[25] This observation is thought to provide reliable understanding of diverse biogeochemical and paleoclimatic applications of the ^{17}O anomalies in stratospheric CO_2, O_2, mineral sulfates, fossil, bones and teeth, which are derived from stratospheric CO_2. The theory of the effect discovered by Thiemens was proposed by Marcus.[26] Isotope fractionation is assumed to arise due to the fact that symmetric (*e.g.*, $^{18}O^{17}O^{18}O$) and asymmetric (*e.g.*, $^{17}O^{18}O^{18}O$) molecules decay at different rates, thus producing isotope discrimination. Robert and Camy-Peret [27] proposed a molecular model in which the same isotope effect is supposed to arise from the competition of scattering and reactive collisions for the molecules with distinguishable and indistinguishable isotopes.

It is worth noting that, physically, it is in fact *mass-dependent* effect; however, due to some specific properties of molecules (see above) it produces isotope fractionation, which deviates from that predicted by the traditional, classical mass-dependent effect. In fact, there are only two, indeed mass-independent isotope effects, the MIE and the NVE; only these two effects will be discussed below.

3. Oxygen isotopes

Oxygen isotopes provide a unique means to monitor the turnover and balance of oxygen in global natural process of its photosynthetic generation and consumption in the oxidation and rotting of organic substances (wood and other plants, micro- and macro-organisms, contaminating oil films and spots on the water of sea and lakes, *etc.*). Oxidation of organic matter by molecular oxygen is the most powerful process fractionating oxygen isotopes. Traditionally, only two isotopes, ^{16}O and ^{18}O, were analyzed and monitored, implying that fractionation of the third isotope, ^{17}O, always obeys the relation $\delta^{17}O \approx 0.5\,\delta^{18}O$. However, by measuring isotope contents in the chain oxidation of various organic compounds by molecular oxygen,[28, 29] it was shown that the fractionation of the magnetic nucleus ^{17}O strongly exceeds that predicted by the relation $\delta^{17}O \approx 0.5\,\delta^{18}O$. Two spin-selective and, therefore, isotope-sorting reactions are responsible for this MIE-induced fractionation, *viz.*, recombination of peroxy radicals and addition of oxygen to alkyl radicals; the former dominates in the oxidation of solids, while the latter prevails in the liquid-state oxidation.

In the oxidation of soft solids, such as polymers, the enrichment of molecular oxygen in the magnetic nuclei ^{17}O was proved to occur in the recombination of peroxy radicals:

$$RO_2^{\bullet} + RO_2^{\bullet} \longrightarrow [ROO^{\bullet}\ {}^{\bullet}OOR] \longrightarrow \longrightarrow ROOOOR \longrightarrow ROOR + O_2 \qquad (2)$$

Here RO_2 are peroxy radicals generated from an organic compound RH. Fractionation proceeds in the radical pair $[ROO^{\bullet}\ {}^{\bullet}OOR]$ formed by encounter of freely diffusing peroxy radicals. The pair may either recombine to give an unstable peroxide ROOOOR, which decomposes releasing two central oxygen atoms as O_2 molecule or dissociates, thus regenerating the peroxy radicals. In the radical pairs formed by encounters of radicals, the ratio of the singlet and triplet state populations is determined by spin statistics and equals 1 : 3. The ^{17}O selection originates from the triplet – singlet conversion of the triplet pairs. Hyperfine coupling on the terminal ^{17}O atoms in peroxy radicals (about 20 G in magnitude [30]) accelerates triplet – singlet conversion of the radical pairs with ^{17}O nuclei and stimulates their recombination. As a result, the peroxide ROOOOR (and, therefore, the regenerated molecular oxygen) should be enriched in the magnetic ^{17}O nuclei; this is in excellent agreement with experiment (Fig. 1).

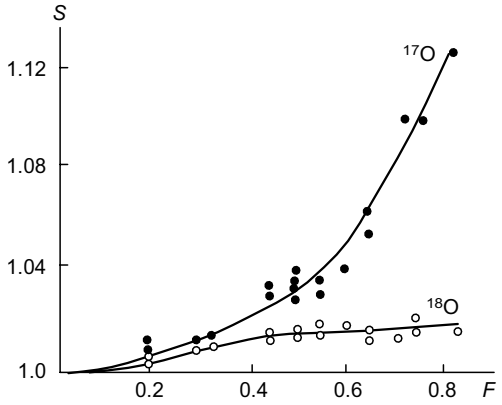


Figure 1. Oxygen ^{17}O and ^{18}O contents (S) as a function of chemical conversion (F) of molecular oxygen in the chain reaction of polymer oxidation. The S values are the ($^{17}O/^{16}O$) ratio for ^{17}O and the ($^{18}O/^{16}O$) ratio for ^{18}O in molecular oxygen.[29]

In the liquid-phase oxidation, another reaction, the addition of oxygen to alkyl radical, is responsible for isotope selection. The encounter of alkyl radical $R^{\bullet}$ with oxygen molecule is followed by the formation of the $(R^{\bullet}\cdots O_2)$ radical pair either in a doublet or quartet spin state (total spin of the pair is 3/2). A peroxy radical as the reaction product is formed only from the doublet pair; quartet – doublet spin conversion induced by the MIE provides nuclear sorting. Electron – nuclear hyperfine coupling in oxygen molecules containing magnetic nuclei ^{17}O stimulates quartet – doublet spin conversion in the encounter pairs $(R^{\bullet}\cdots O_2)$ [31] and accelerates the addition reaction. It depletes molecular oxygen of magnetic nuclei (Fig. 2); the ratio of the addition rate constants $k(^{17}O^{16}O)/k(^{16}O^{16}O)$ was found to be 1.011, *i.e.*, the $^{17}O^{16}O$ molecules react 1.1% faster than the $^{16}O^{16}O$ molecules.

The MIE was shown to fractionate oxygen isotopes in the photooxidation of water by molecular oxygen.[32] Photolysis of $^{17,18}O$-labelled water in the presence of molecular oxygen is accompanied by transfer of the ^{17}O and ^{18}O isotopes from water to oxygen, thus demonstrating that the photoinduced oxidation of water does occur. The reaction exhibits MIE, namely, the oxidation of $H_2{}^{17}O$ is

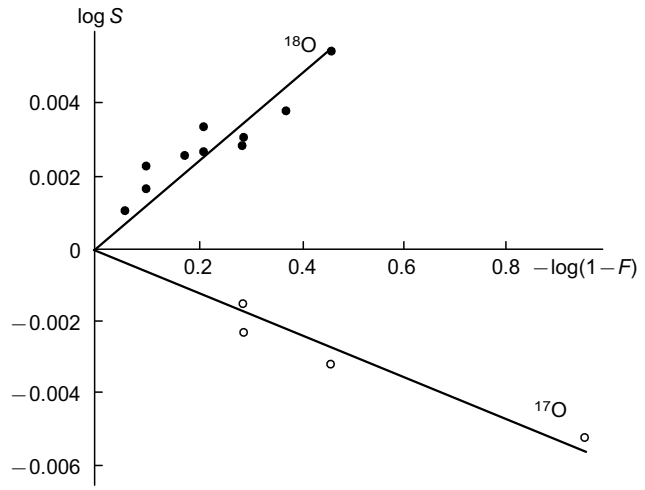


Figure 2. Isotope composition of molecular oxygen as a function of its chemical conversion in the chain oxidation of ethylbenzene (Hereinafter *S* and *F* are the same as in Fig. 1).[31]

3.3% faster (in the Earth magnetic field) and 3.7% faster (in a magnetic field of 0.5 T) than the oxidation of $H_2{}^{18}O$. The key reaction producing fractionation of oxygen isotopes is supposed to be the recombination of the HO_2 radicals. Photooxidation of water by molecular oxygen is thought to be important for the elucidation of global processes of oxygen production and consumption in Nature;[33–35] this can be best done by monitoring the isotopic composition. Moreover, the oxygen–water photoinduced reaction is in a focus of two problems: first, the ecology of natural water related to the synthesis of hydrogen peroxide under sunlight and, second, atmospheric photoinduced nucleation of water vapour into nanodroplets and fog formation.

Mass-independent fractionation of oxygen isotopes in hydrogen peroxide formed upon dissociation of water vapour induced by discharge results in enrichment of the peroxide in ^{17}O by 1.4‰ in the absence of O_2 and by 2.5‰ in the presence of O_2.[36] The observed MIE seems to originate from the recombination of HO and HO_2 radicals in H_2O nanodroplets (similar to recombination of peroxy radicals as discussed above). These results are sought to be important in atmospheric chemistry.

A remarkable effect was discovered by Miller *et al.*[37–39] Thermally induced decomposition of many metal carbonates was found to produce anomalous fractionation of magnetic isotope ^{17}O in the reaction products, *viz.*, the solid oxide appears to be depleted of ^{17}O, while CO_2 is enriched in ^{17}O to the same extent. The key step of the reaction mechanism is supposed to be electron transfer, which generates a radical pair in the singlet spin state S:

$$(M^{2+}CO_3^{2-})^S \longrightarrow (M^{2+}CO_3^-)^S \qquad (3)$$

where M = Ca, Mg, Ba, *etc.* In this radical pair, spin-allowed back electron transfer may occur, which regenerates the starting reactants. However, the pairs with ^{17}O nuclei experience spin conversion into the triplet state T, in which back electron transfer is spin-prohibited, so that these pairs predominantly release CO_2 enriched in ^{17}O:

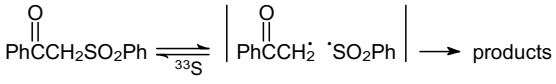
$$(M^{+}{}^{17}OCO_2^-)^S \longrightarrow (M^{+}{}^{17}OCO_2^-)^T \longrightarrow (M^{+}{}^{17}OCOO^-)^T \longrightarrow {}^{17}OCO + (M^+O^-)^T \qquad (4)$$

Magnetically induced fractionation of oxygen isotopes is supposed to be important in geochemistry and mineralogy as a means to decipher and understand the reaction mechanism by monitoring the isotopic composition of rocks and deposits and to reproduce their chemical genesis and evolution.

4. Magnetic isotopes of sulfur

In the sulfur isotope triad $^{32}S-{}^{33}S-{}^{34}S$, only one nucleus is magnetic, namely, ^{33}S has a nuclear spin of 3/2 and a magnetic moment of 0.64 μ_B. Isotope fractionation induced by ^{33}S-MIE was first observed in the photolysis of a sulfur-containing ketone (Scheme 1).[40]

Scheme 1



Photolysis generates an excited ketone in the triplet spin state, which creates a triplet radical pair. The latter sorts isotopes, *viz.*, the pairs with magnetic ^{33}S nuclei undergo the fast triplet–singlet conversion and recombine, thus regenerating the ketone. The triplet–singlet conversion of pairs with the ^{32}S and ^{34}S nuclei is delayed and they predominantly dissociate into separated radicals, which produce reaction products.

The sulfur isotope content in the ketone as function of its chemical conversion is shown in Fig. 3. Evidently, the regenerated ketone accumulates ^{33}S nuclei; its enrichment greatly exceeds that of ^{34}S, firmly demonstrating the MIE. This mechanism of isotope fractionation was unambiguously proved by the observation of chemically induced dynamic nuclear and electron polarization (well known CIDNP and CIDEP, respectively) as well as by the detection of the magnetic field effect on the reaction rate.[41]

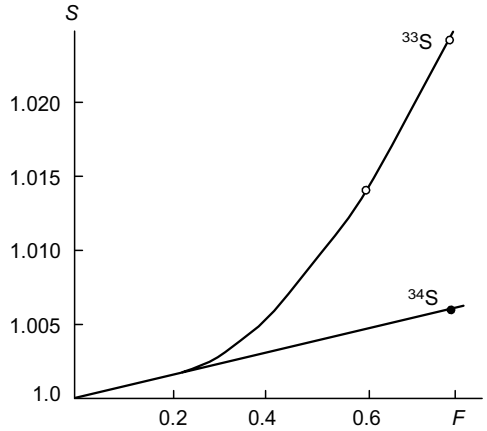


Figure 3. Sulfur isotope fractionation induced by photolysis of sulfur-containing ketone as function of its chemical conversion.[41]

More recently, the ^{33}S-MIE was confirmed in the photo-induced dissociation of *p*-aminophenyl disulfide (Scheme 2).[42]

Scheme 2

$$(H_2NPhS)_2 \underset{^{33}S}{\rightleftharpoons} \left| H_2NPhS^{\bullet} \quad {}^{\bullet}SO_2Ph \right|^{T} \longrightarrow \text{products}$$

The triplet radical pair acts as spin-selective nanoreactor which fractionates isotopes; it returns radicals with the magnetic ^{33}S nuclei into the regenerated starting disulfide. The dependence of the fractionation coefficient α (Fig. 4) on the magnetic field leaves no doubt in the ^{33}S-MIE fractionation.

The MIE was certainly observed in thermochemical sulfate reduction;[43] the large ^{33}S enrichment (13‰), beyond what would be expected from the mass-dependent effect, was detected in the polysulfide fraction of products. This effect is thought to contribute substantially to the Archean sulfur isotope anomalies observed in geochemistry.

Thermochemical sulfate reduction reactions are of special interest in Earth and environmental chemistry. Anomalously fractionated sulfur isotopes in many sedimentary rocks older than 2.4 billion years were widely thought to be the products of UV photolysis of volcanic sulfur dioxide in an anoxic atmosphere. Watanabe *et al.*[44] demonstrated that high-temperature reduction of sulfate using amino acids as organic substrates exhibits mass-independent sulfur isotope fractionation. In the laboratory experiments it was shown that reduced sulfur species produced by the dark reactions between powders of amino acids and sulfate at 150 to 200 °C, possess anomalous sulfur-33 isotope contents: $\Delta^{33}S = +0.1‰$ to $+2.1‰$. These results suggest that reactions between organic matter in sediments and sulfate-rich hydrothermal solutions may produce anomalous sulfur isotope signatures in some sedimentary rocks and may be related to the thermal and biological evolution of the Earth.

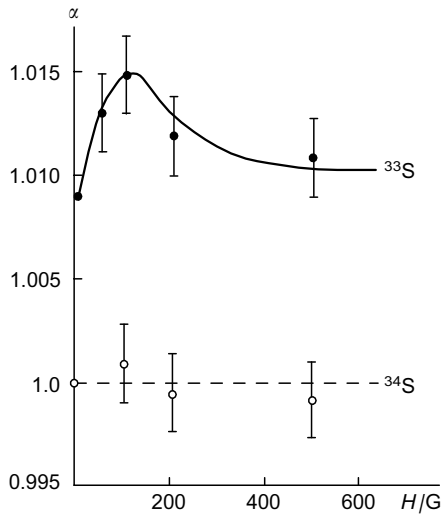


Figure 4. Magnetic field dependence of the one-step enrichment coefficient α for the fractionation of sulfur isotopes.[53]
Fractionation of ^{33}S is controlled by MIE and depends on the magnetic field; fractionation of ^{34}S is controlled by mass-dependent isotope effect and is independent of the magnetic field.

The most impressive results were reported by Oduro *et al.*[45] Prolonged heating of sodium sulfate with powdered glycine (300 °C for 340 h) was shown to produce Cr-reducible sulfur and hydrogen sulfide, which were enormously, by 10‰, both enriched in ^{33}S. A well-founded mechanism was suggested, which explains both products and isotope anomaly. It implies that the observed isotope effect originates from the intermediate radical-ion pair $(RS^{\bullet}H^{+}/RS^{\bullet}SH)^{-}$ which is formed by electron transfer between RSH as an electron donor and RSSH as an acceptor.

Besides the reactions proposed by Oduro *et al.*[45] other reactions may be suggested. Glycine in the ionic form $NH_3^+CH_2CO_3^-$ can withdraw an electron from SO_4^{2-} (or HSO_4^{2-}) to give the $NH_3^{\bullet}CH_2CO_2^-$ radical, which decomposes into NH_3 and ${}^{\bullet}CH_2CO_2^-$ radical *via* N–C bond scission. The alkyl radical may abstract a hydrogen atom from glycine

$$ {}^{\bullet}CH_2CO_2^- + NH_2CH_2CO_2H \longrightarrow \quad (5)$$

$$\longrightarrow CH_3CO_2^- + NH_2CH^{\bullet}CO_2H$$

thus producing a new radical. Both alkyl radicals (we will denote them as R$^{\bullet}$) may add to SO_4^{2-} (or HSO_4^{2-}) anion yielding a new sulfur-containing radical which decomposes by β-scission of the S–O bond:

$$R^{\bullet} + SO_4^{2-} \longrightarrow (ROSO_3^{2-})^{\bullet} \quad (6)$$

$$(ROSO_3^{2-})^{\bullet} \longrightarrow RO^{\bullet} \rightarrow SO_3^{2-} \quad (7)$$

The addition of alkyl radicals to SO_3^{2-} will consecutively transform the SO_3^{2-} anion into SO_2^{2-}, SO^{2-} and, finally, S^0. Alkoxyl radicals RO$^{\bullet}$ generate alkyl radicals by hydrogen atom abstraction; finally, this sequence of reactions is in fact a chain radical process. Under aerobic conditions, the participation of sulfur-containing peroxy radicals $RSOO^{-}$ also cannot be excluded.[30]

These chain reactions can be accompanied by yet another process, namely, electron transfer from $NH_2CH_2CO_2^-$ to H_3O^+ or $H_5O_2^+$ (Zundel cation) producing HO$^{\bullet}$ and $NH_2CH_2CO_2^{\bullet}$ radicals; the latter almost instantly releases CO_2 and an alkyl radical $NH_2CH_2^{\bullet}$. Both the alkyl radical and HO$^{\bullet}$ are involved in the hydrogen abstraction reaction. The sulfur-containing radical can also abstract hydrogen atoms, finally generating H_2S. Fractionation of ^{33}S occurs by the MIE in the encounter radical pairs with sulfur-containing radicals as partners. The spin relaxation times of these radicals are rather long and cannot disturb or prevent coherent triplet – singlet spin conversion as a source of the MIE. This statement was unambiguously proved by the observation of the ^{33}S-MIE and CIDNP[41] (see above).

Mass-independent sulfur isotope fractionation was detected in sulfur-bearing phases from 13 carbonaceous chondrites.[46] The largest effect with $\Delta^{33}S$ values between 0.104‰ and 0.256‰ is exhibited by S^0; it was suggested that mass-independent fractionation arises from H_2S photodissociation in the nebula. The $\Delta^{33}S$ values in sulfide and sulfate are correlated with those for S^0; this indicates a genetic relationship between the S-bearing phases.

5. Iron isotopes

The chemical behaviour of iron isotopes is most important for understanding metabolic biomineralization of intracellular magnetite (Fe_3O_4) nanoparticles, which occur in living organisms in special organelles called magnetosomes. This process is known to be performed by magnetotactic bacteria. Although they may be the earliest microorganisms capable of biomineralization on Earth, identification of their activity in ancient sedimentary rocks remains intriguing and needs isotopic biosignature. Recently, Fe isotope fractionation by the magnetotactic bacterium *Magnetospirillum magneticum* was discovered by Amor *et al.*[47] This bacterium was shown to produce magnetite depleted of heavy Fe isotopes by 1.5‰ to 2.5‰ relative to the initial growth medium. Moreover, mass-independent isotope fractionation in magnetic ^{57}Fe during magnetite biomineralization was observed ($\Delta^{57}Fe = +0.23‰$), but not in the nonmagnetic isotopes ^{54}Fe, ^{56}Fe and ^{58}Fe as evidence of the MIE. Amor *et al.*[47] suggested that this Fe isotope anomaly provides a potential biomarker for the identification of magnetite produced by ancient magnetotactic bacteria in geological record.

The MIE-induced anomalous enrichment of magnetite with ^{57}Fe is proposed to be generated during the reduction of Fe^{III} into Fe^{II} by cytochromes or other redox enzymes. It implies that the spin transition in the radical-ion pair $[Fe^{II}L^{\bullet +}]$ created by electron transfer between Fe^{III} and the reducing molecule L is notably induced by hyperfine coupling with the nuclear magnetic moment of ^{57}Fe. In the $[Fe^{II}L^{\bullet +}]$ pair, back electron transfer is spin-allowed and regenerates the Fe^{III} ion. The direct reaction generating a product is supposed to be spin-forbidden, but hyperfine coupling with ^{57}Fe partly allows this process. As a result, Fe^{II} ions and magnetite accumulate the ^{57}Fe nuclei.

However, Fe^{II} is a high-spin ion with very short electron relaxation time (it is much shorter that the time of spin conversion induced by hyperfine coupling). Fast relaxation in this ion may prevent coherent spin conversion in the $[Fe^{II}L^{\bullet +}]$ pair and destroy the MIE. The possible way out of this contradictory situation is to assume that the coordination of ions by ligands in enzymatic site is such that it modifies structure of electron levels and delays spin relaxation in pair $[Fe^{II}L^{\bullet +}]$, although this assumption remains to be speculative.

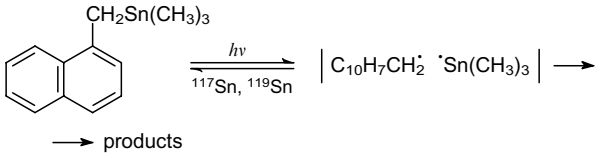
A series of laboratory studies on iron and oxygen isotope fractionation during intracellular production of magnetite by the magnetotactic bacteria *Magnetospirillum magnetotacticum* and *Magnetovibrio blakmorei* was reported.[48] No detectable fractionation of iron isotopes in the bacterial magnetite was observed. However, the ^{18}O isotope exhibited temperature-dependent fractionation between Fe_3O_4 and water, thus demonstrating normal mass-dependent isotope effect. The contradictory results[47,48] are discouraging and intriguing; no certain conclusions can be made. It is appropriate to remind the ^{57}Fe-NVE analysis by Fujii *et al.*[49] who showed that the nuclear volumes of all iron isotopes almost linearly depend on the nuclear mass, so that the NVE is expected to be small and hardly detectable even with a high-precision analysis.

Isotopic analyses of granite and mineral separated from the Renison tin deposit in western Tasmania detected fractionation of iron isotopes, *viz.*, pyrite, magnetite and chalcopyrite were isotopically heavier than pyrrhotite and siderite.[50] The ratio $\delta^{56}Fe = 0.68\,\delta^{57}Fe$ seems to indicate an equilibrium fractionation resulting from mass-dependent isotope effect.

6. Tin and germanium isotopes

Magnetic isotopes of Sn and Ge may be useful in geology as indicators of the genesis and geochemical evolution of ores. Among tin isotopes, the most important are the magnetic ones, ^{117}Sn (spin 1/2, magnetic moment 1.0 μ_B) and ^{119}Sn (spin 1/2, magnetic moment 1.046 μ_B). The evidence of the MIE for the tin nuclei was first obtained[51] in the photolysis of (1-naphthylmethyl)trimethyltin (Scheme 3).

Scheme 3



The radical pair formed by photodissociation of the C–Sn bond can either regenerate the starting reactant by recombination or dissociate. The radicals escaping the pair undergo dimerization to yield the major products, hexamethyldistannane $(CH_3)_3SnSn(CH_3)_3$ and dinaphtylethane $(C_{10}H_7CH_2)_2$. The contents S of the magnetic nuclei ^{117}Sn and ^{119}Sn as a function of the chemical conversion F are shown in Fig. 5 in terms of the equation[51,52]

$$\log S = \frac{1-\alpha}{\alpha}\log(1-F) \qquad (8)$$

where α is the one-step enrichment coefficient. Photolysis is evident to enrich the starting compound in the magnetic nuclei ^{117}Sn and ^{119}Sn ($S > 1$), whereas the product, hexamethyldistannane, is depleted of them ($S < 1$). It is clear that the initial radical pair is formed in the triplet state; triplet–singlet conversion of the pairs containing the ^{117}Sn and ^{119}Sn nuclei is induced by hyperfine coupling in the

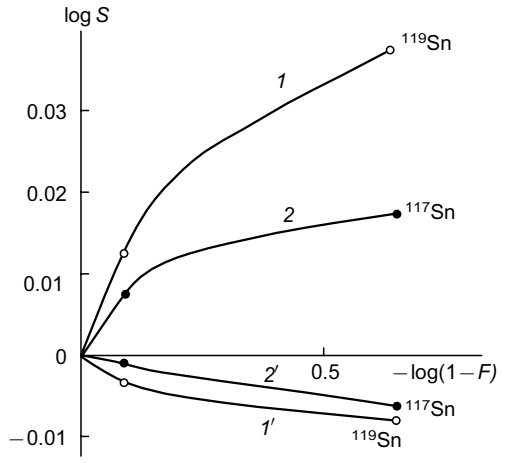
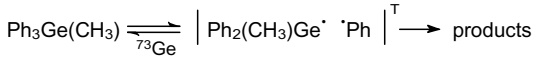


Figure 5. The tin isotope composition S of (1-naphthylmethyl)trimethyltin (*1*, *2*) and hexamethyldistannane (*1′*, *2′*) as a function of chemical conversion F (both are in the logarithm scale).[51,52]

$^{\bullet}Sn(CH_3)_3$ radical [coupling constants $a(^{117}Sn)$ and $a(^{119}Sn)$ are equal to 1536 G and 1607 G, respectively].[52] Fast spin conversion returns these pairs back into the starting molecule, while spin conversion in the pairs containing nonmagnetic nuclei is delayed and allows the radicals to escape and bring the ^{116}Sn and ^{118}Sn nuclei into the product, hexamethyldistannane.

The magnetic nucleus ^{73}Ge (spin 9/2, magnetic moment 0.88 μ_B) also exhibits the MIE which was for the first time observed in the photolysis of methyltriphenylgermane.[53] The photolytic reaction produces a radical pair in the triplet state (Scheme 4).

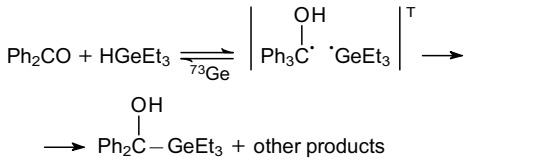
Scheme 4



Hyperfine coupling in the germyl radical (coupling constant of about 80 G)[53] induces fast triplet – singlet conversion of the pair and returns the magnetic ^{73}Ge nuclei into the initial compound, which accumulates them. The plots of the one-step enrichment coefficients α *vs.* magnetic field shown in Fig. 6 provide an unambiguous signature of the MIE.

Similarly, ^{73}Ge isotope fractionation was stimulated by the photochemical reaction between triplet-excited benzophenone and triethylgermane in sodium dodecyl sulfate micelles (Scheme 5).[54]

Scheme 5



Again hyperfine coupling in the $GeEt_3$ radical transforms the triplet radical pair into a singlet one which recombines faster if it contains the magnetic ^{73}Ge nuclei,

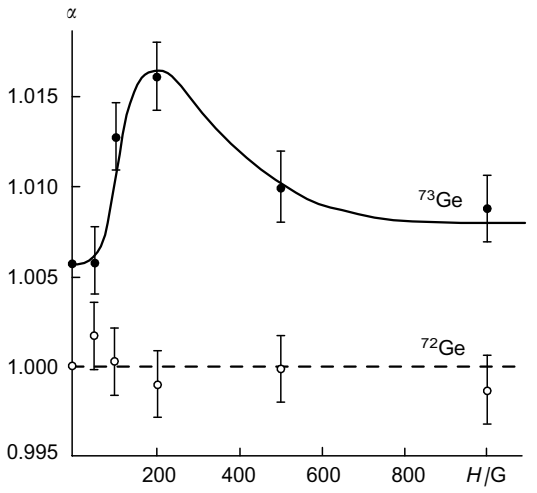


Figure 6. One-step enrichment coefficients α as function of magnetic field in the photolysis of methyltriphenylgermane.[53]

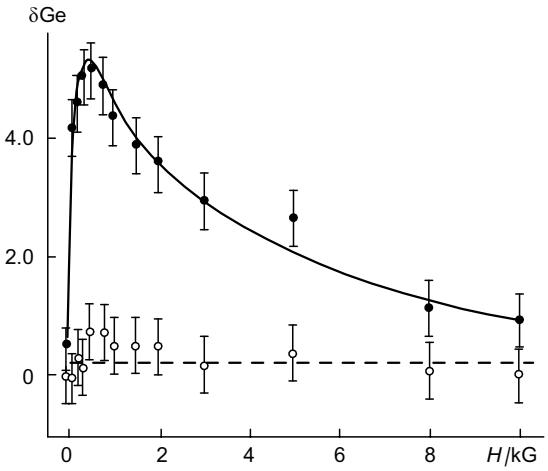


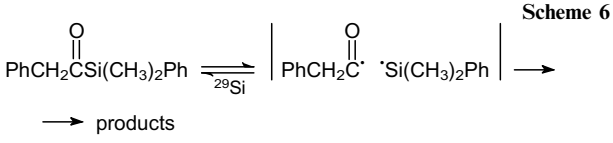
Figure 7. Isotope enrichments in germyl carbinol for ^{73}Ge (solid circles) and ^{72}Ge (open circles) as function of magnetic field (δGe values are given in per mille).[54]

resulting in the accumulation of ^{73}Ge in the initial compound. The magnetic field dependence of ^{73}Ge and ^{72}Ge isotope fractionation in terms of the δGe magnitudes shown in Fig. 7 clearly proves the magnetic nature of isotope sorting and demonstrates tremendous superiority of the MIE over the classical effect.

7. Magnetic isotopes of silicon

Silicon magnetic isotope may be also useful in geology as an indicator of geochemical evolution of ores. In the $^{28}Si - ^{29}Si - ^{30}Si$ isotopic triad, only the ^{29}Si nucleus is magnetic (spin 1/2, magnetic moment 0.555 μ_B); its magnetic field produces fractionation of magnetic and nonmagnetic silicon isotopes. It was detected in the photolysis of benzyl silyl ketone $PhCH_2C(O)Si(CH_3)_2Ph$ (Scheme 6).[55]

Scheme 6



The radical pair generated in this reaction unexpectedly appeared to be in the singlet spin state; as a concequence, the regenerated ketone is impoverished in the magnetic isotope (Fig. 8, line *2*). Photolysis of the same ketone sensitized by acetophenone (a triplet sensitizer) led to reversal of the MIE sign, now ketone was considerably enriched in the magnetic ^{29}Si isotope (Fig. 8, line *1*). A small enrichment of the ketone in nonmagnetic ^{30}Si is determined by the mass-dependent fractionation; it does not depend on the starting multiplicity, being the same for both singlet and triplet states of the initial ketone (see Fig. 8).

The oxidation of silicon crystals by molecular oxygen also demonstrates the ^{29}Si-MIE: silicon atoms containing ^{29}Si are oxidized twice faster than atoms containing spinless, nonmagnetic nuclei ^{28}Si and ^{30}Si (Fig. 9);[56] this effect

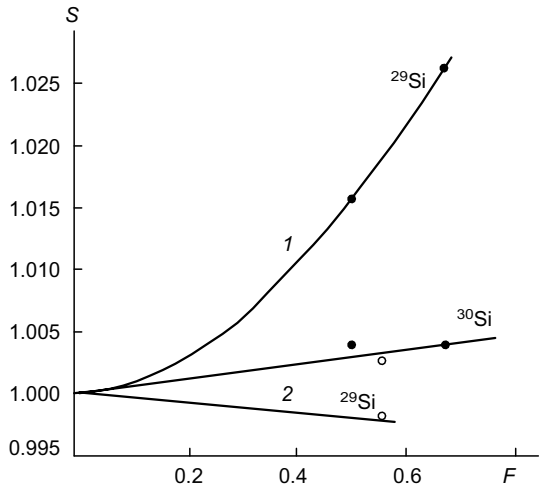


Figure 8. Silicon isotope fractionation induced by photolysis of benzyl silyl ketone as a function of chemical conversion (data taken from Ref. 55).
Mass-dependent fractionation of ^{30}Si is identical for the direct (*1*) and sensitized (*2*) photolysis. The MIE-induced ^{29}Si isotope separation depends on the spin multiplicity.

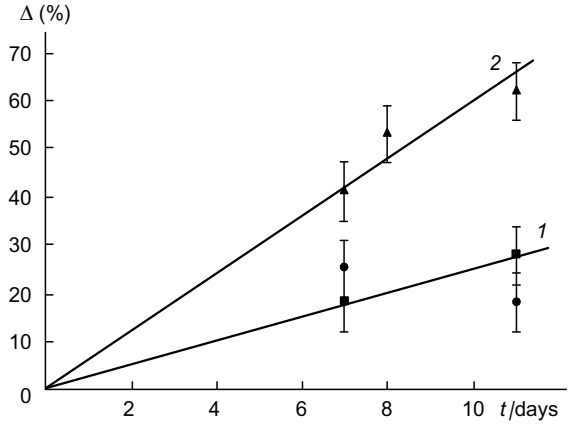


Figure 9. The yield Δ of silicon oxidation products (in arbitrary units) as a function of time for nonmagnetic nuclei ^{28}Si (circles) and ^{30}Si (squares) (*1*), and for magnetic ^{29}Si (triangles) (*2*).[56]

supports the radical pair mechanism for solid-state silicon oxidation.

8. Uranium isotopes

Uranium isotope fractionation in the photolysis of uranyl salts in the presence of a substituted phenol PhOH and NH_4F was reported.[57] The photoinduced reaction

$$UO_2^{2+} + PhOH \underset{^{235}U}{\overset{h\nu}{\rightleftharpoons}} [UO_2H^{\bullet}\ {}^{\bullet}OPh]^{T} \xrightarrow[^{238}U]{} UO_2H^{\bullet} + PhO^{\bullet} \quad (9)$$

generates a triplet radical pair $[UO_2H^{\bullet}\ {}^{\bullet}OPh]^{T}$, which undergoes fast triplet–singlet conversion if it contains magnetic ^{235}U nuclei; then, spin-allowed reverse hydrogen atom transfer in the singlet pair regenerates phenol and the uranyl ion UO_2^{2+} enriched in magnetic ^{235}U nuclei. Triplet–singlet conversion of the pairs with nonmagnetic ^{238}U nuclei delays and the escaping radicals carry the ^{238}U nuclei into the ultimate reaction product UF_4. The starting uranyl salt therefore accumulates the ^{235}U magnetic nuclei.[57] It is worth keeping in mind that similar dark geochemical reactions may occur at elevated temperatures and result in inversion of the sign of ^{238}U-MIE and isotope fractionation.

9. Mercury isotopes

Mercury is a well-known environmental pollutant, especially in its organic forms, which has posed serious risks for human health; the sources and pathways of its biogeochemical cycle are still not yet completely understood. Measurement of stable isotope composition is supposed to be a powerful and possibly the only means to distinguish and monitor this hazardous pollutant. Mercury has seven stable isotopes, of which the odd isotopes ^{199}Hg and ^{201}Hg have nonzero spins and magnetic moments, while all even isotopes are spinless and non-magnetic. Spin conversion of radical pairs is controlled by hyperfine coupling of the unpaired electrons with mercury magnetic nuclei. The coupling constants are known for some radicals, such as CH_3Hg (1758 G), HgH (2450 G), $(CH_3)_2Hg^+$ (2674 G);[58] these values refer to ^{199}Hg but can be easily converted to those of ^{201}Hg.

MIE-induced fractionation of ^{199}Hg was for the first time detected[59] in the photolysis of bis(*p*-trifluoromethylbenzyl)mercury resulting in 1,2-bis(*p*-trifluoromethylbenzyl)ethane and metallic mercury. Figure 10 shows that the absolute abundance of ^{199}Hg (measured by NMR as the intensities of satellite lines) in bis(*p*-trifluoromethylbenzyl)-mercury remaining after partial photolysis increases in the course of the reaction, namely, the content of ^{199}Hg increases by 4% at a conversion of about 50%.

The composition of the products and the isotope fractionation are satisfactorily described by the following Scheme 7.

Isotope sorting occurs in the triplet radical pair formed upon C–Hg bond dissociation in the triplet excited molecule. The pairs with ^{199}Hg nuclei rapidly evolve from the triplet to singlet state and recombine, returning magnetic nuclei into the starting molecule. The triplet–singlet conversion of pairs with the nonmagnetic even nucleus (^{200}Hg, ^{202}Hg) delays and these pairs dissociate into separated radicals and then react to give products, 1,2-bis(*p*-trifluoro-

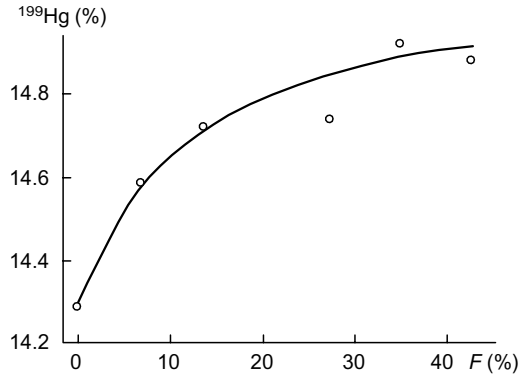


Figure 10. ^{199}Hg isotope content in bis(*p*-trifluoromethylbenzyl)-mercury as a function of its chemical conversion.[59]

Scheme 10

$$(CF_3C_6H_4CH_2)_2Hg \underset{^{199}Hg}{\overset{h\nu}{\rightleftharpoons}} {}^3(CF_3C_6H_4\dot{C}H_2\ \dot{H}gCH_2C_6H_4CF_3) \xrightarrow{^{200}Hg} CF_3C_6H_4\dot{C}H_2 + \dot{H}gCH_2C_6H_4CF_3 \longrightarrow (CF_3C_6H_4CH_2)_2 + Hg$$

methylbenzyl)ethane and metallic mercury. Thus, the radical pair, being an electron and nuclear spin-selective nanoreactor, acts as a molecular device that fractionates isotopes.

The starting bis(*p*-trifluoromethylbenzyl)mercury is enriched in ^{199}Hg isotope under the conditions when emulsion of colloidal mercury precipitated and photolysis occurred in transparent solutions. However, continuous photolysis of solutions with colloidal mercury led to depletion of bis(*p*-trifluoromethylbenzyl)mercury in the ^{199}Hg isotope. Such an inversion of the sign of the isotope effect provides an unambiguous proof that under these conditions, photolysis of bis(*p*-trifluoromethylbenzyl)mercury is sensitized by atomic mercury; it occurs in the singlet excited state and generates a singlet radical pair in which the direction of spin conversion and isotope selection change the sign;[60] inversion of the MIE sign is incompatible with NVE.

Nuclear spin-dependent fractionation of mercury isotopes was detected in the photoreduction of Hg^{2+} and photodegradation of MeHgX in aquatic systems;[61] the magnitudes of fractionation were estimated by the equations

$$\Delta^{199}Hg \approx \delta^{199}Hg - 0.2520\,\delta^{202}Hg \quad (10)$$

$$\Delta^{201}Hg \approx \delta^{201}Hg - 0.7520\,\delta^{202}Hg \quad (11)$$

similar to Eqn (1). Photochemical reduction by natural sunlight was shown to result in dramatic accumulation (up to 2.5‰) of magnetic nuclei ^{199}Hg and ^{201}Hg in the starting reactants (Fig. 11), which unambiguously indicates that the photoreduction is a radical reaction; the following schemes may be suggested for the reaction:

$$MeHgX \underset{^{199}Hg,\ ^{201}Hg}{\overset{h\nu}{\rightleftharpoons}} [\dot{M}e\ \dot{H}gX]^T \longrightarrow \text{products (including } Hg^0) \quad (12)$$

$$Hg^{2+} + Y \underset{^{199}Hg,\ ^{201}Hg}{\overset{h\nu}{\rightleftharpoons}} [Hg^+\ Y^+]^T \longrightarrow \text{products} \quad (13)$$

Here X is a substituent at MeHg (unknown but any) and Y is a reactant (unknown). Both MeHgX and Hg^{2+} react in excited triplet spin states and generate triplet radical pairs. These pairs with magnetic nuclei undergo fast triplet – singlet spin conversion and return the magnetic nuclei into the reactants. It was also found that fish displays a large excess (up to 4‰) of magnetic nuclei ^{201}Hg over nonmagnetic ^{202}Hg. This was interpreted as evidence that fish accumulates mostly MeHgX and that a majority (> 80%) of Hg present in fish muscle is MeHgX. These outstanding results convincingly demonstrate that mercury isotopes can be successfully used as the tracers of the Hg biogeochemical pathways in the environment.

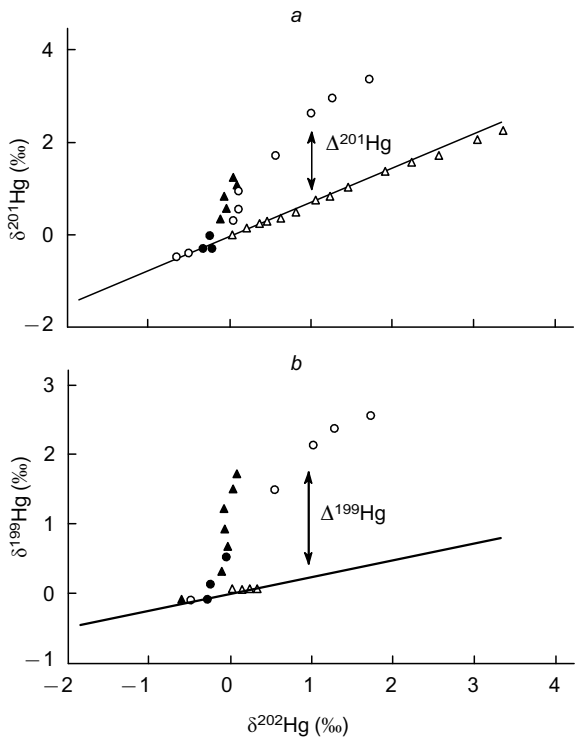


Figure 11. The relationship between isotope shifts δ^{201}Hg (*a*) and δ^{199}Hg (*b*) for magnetic nuclei and δ^{202}Hg for nonmagnetic nucleus in photoinduced reactions.[61]

There are many observations of mercury isotope fractionation: in coal combustion and sea water flue gas desulfurization,[62] in the roasted ore waste,[63] in atmospheric fine particles as a result of surface chemistry,[64] in hydrothermal systems in the Yellowstone Plateau volcanic field and Guaymas rift,[65] in coal and oil-fired utilities,[66] in photoreduction of organic carbon dissolved in natural water[67] and in many other processes and objects including those in the fault earthquake region.[68, 69]

10. A test: MIE or NVE?

For heavy elements, both mass-independent isotope effects, MIE and NVE, are supposed to coexist; however, a careful analysis of many experimental results indicates that the contribution of the NVE to isotope fractionation, produced by reactions themselves, is hardly important, or is at least ambiguous. On the opposite, NVE dominates in nonchemical processes.[70] In contrast to the MIE-induced bidirectional fractionation, the NVE induces a unidirectional, universal isotope fractionation that is almost independent of the reaction mechanism; it is incompatible with the inversion of the fractionation sign.[12, 71]

It is worthwhile to formulate a criterion for differentiation of these two effects. A decisive test comes from physics; it will be illustrated taking mercury nuclei as an example. Both nuclei, ^{201}Hg and ^{199}Hg, are magnetic (their magnetic moments are -0.50 and $+0.56$ μ_B, respectively). The rate of coherent triplet – singlet conversion is controlled by the hyperfine coupling constant *a*:

$$a = (8\pi/3)\mu_e\mu_n|\Psi(0)|^2 \quad (14)$$

Here μ_e and μ_n are the magnetic moments of electron and nucleus, respectively, and $|\Psi(0)|^2$ is the spin density of the s electron at the nucleus. The ratio $\Delta^{201}Hg/\Delta^{199}Hg$ is determined by ratio of a (*i.e.* of μ_n) and depends on the lifetime τ of the radical pair.[9] For short-lived pairs ($\tau < a^{-1}$), the rate of triplet–singlet conversion is limited by spin dephasing; then

$$\Delta^{201}Hg/\Delta^{199}Hg = ({}^{201}\mu_n/{}^{199}\mu_n)^2 = 1.25 \quad (15)$$

For long-lived pairs ($\tau > a^{-1}$), the spin state oscillates between triplet and singlet; then

$$\Delta^{201}Hg/\Delta^{199}Hg = ({}^{201}\mu_n/{}^{199}\mu_n)^{1/2} = 1.05 \quad (16)$$

If isotope fractionation is controlled by the MIE, the ratio $\Delta^{201}Hg/\Delta^{199}Hg$ is expected to be in the range of 1.05–1.25; if isotope fractionation is controlled by the NVE, the ratio $\Delta^{201}Hg/\Delta^{199}Hg$ is estimated to be in the range of 0.50–0.62 (Ref. 71) (uncertainty corresponds to that in nuclear volumes). Experimental values of the ratio $\Delta^{201}Hg/\Delta^{199}Hg$ in different reactions of mercury-containing species were summarized by Ghosh *et al.*[72] Most of them are equal to 1.11 and thus fall in the range of 1.05–1.25.

It is worth noting that MIE-induced isotope fractionation is independent of the nuclear spin. Again, this is easy to understand using the ^{201}Hg and ^{199}Hg nuclei as examples. Their spins I are different: 3/2 and 1/2, respectively. In the case of ^{201}Hg, triplet–singlet conversion proceeds through four nuclear spin channels ($2I + 1 = 4$), but the population of each channel is four times lower. In the case of ^{199}Hg, triplet–singlet conversion proceeds through two nuclear spin channels ($2I + 1 = 2$), but the population of each channel is two times lower. In both cases, the normalized populations are equal to unity. Finally, the total rates of triplet–singlet conversion appear to be almost equal for both nuclear spins.

It is necessary to mention the factors preventing isotope fractionation. Nuclear selection is controlled by coherent spin conversion, which occurs as a spin dephasing of unpaired electrons of the partners in the pair of spin carriers. Another process that competes with coherent dephasing is noncoherent, stochastic electron spin relaxation, which is mainly controlled by intramolecular spin–orbit coupling; the latter process suppresses coherently induced nuclear fractionation. However, the destroying function of this coupling is strongly exaggerated: even radicals containing heavy atoms in which the spin–orbit coupling is known to be significant (such as mercury, tin, germanium, and even uranium) reliably exhibit coherent dephasing and MIE-induced fractionation. It follows that spin–orbit coupling is not the critical factor preventing isotopic fractionation.

11. Chemical scenarios of MIE-induced mercury isotope fractionation

The MIE-induced isotope fractionation begins with the formation of radical (or radical-ion) pairs by electron or hydrogen atom transfer, or by a dissociation reaction. Now we will discuss the main mechanisms of radical pair generation and isotope sorting in these pairs.

In Scheme 11 the donor D is implied to be SO_4^{2-}, SO_3^{2-}, HO_2^-, metal cations (Fe^{2+}, Mn^{2+}, Co^{2+}), RS^- anions, carboxylic acid (including amino acid) anions RCO_2^-, HO^- anion, or any organic molecule as an electron or hydrogen atom donor. Photolysis is supposed to generate a radical pair in the triplet state, which is not able to regenerate the starting reactants due to spin forbiddenness. However, hyperfine coupling in pairs with magnetic nuclei $^{199,201}Hg$ stimulates triplet–singlet spin conversion and transforms the triplet pairs into singlet ones; the latter regenerate the starting reactants and return the magnetic nuclei into the initial mercury compound. As shown above (see Section 10), the isotope ratio $\Delta^{201}Hg/\Delta^{199}Hg$ in it is expected to lie between 1.05 and 1.25, while the products are depleted of these nuclei in the ratio $\Delta^{201}Hg/\Delta^{199}Hg = 0.80–0.95$.

Scheme 11

$$Hg^{2+} + D \underset{{}^{199}Hg,\ {}^{201}Hg}{\overset{h\nu}{\rightleftharpoons}} [Hg^{+\bullet}\ D^{+\bullet}]^T \xrightarrow[{}^{200}Hg,\ {}^{202}Hg]{} \text{products}$$

$$\Delta^{201}Hg/\Delta^{199}Hg = 1.05–1.25 \;||\; \Delta^{201}Hg/\Delta^{199}Hg = 0.80–0.95$$

$$Hg^{2+} + D \underset{{}^{200}Hg,\ {}^{202}Hg}{\overset{kT}{\rightleftharpoons}} [Hg^{+\bullet}\ D^{+\bullet}]^S \xrightarrow[{}^{199}Hg,\ {}^{201}Hg]{} \text{products}$$

$$\Delta^{201}Hg/\Delta^{199}Hg = 0.80–0.95 \;||\; \Delta^{201}Hg/\Delta^{199}Hg = 1.05–1.25$$

These predictions are in accordance with experiment, *viz.*, the residual Hg^{2+} is enriched in ^{199}Hg, ^{201}Hg in a $\Delta^{201}Hg/\Delta^{199}Hg$ ratio of about 1;[71] in biological systems this ratio is found to be 1.11.[72] However, in some experiments this ratio deviates from the expected values and lies in the range of 1.0–0.75;[61,67] the reasons for these deviations will be discussed later.

Thermally induced reactions are supposed to be responsible for the regeneration of volatile mercury compounds from deposits in the dark reactions; they are expected to generate radical pairs in the singlet state (Scheme 1) in which singlet–triplet conversion stimulates the formation of products enriched in magnetic nuclei, while the starting reactants are depleted of these isotopes. Inversion of the spin multiplicity results in the inversion of the MIE sign, namely, now one has $\Delta^{201}Hg/\Delta^{199}Hg = 1.05–1.25$ in products and $\Delta^{201}Hg/\Delta^{199}Hg = 0.80–0.95$ in the starting reactants; it is opposite to what is observed in the photoreduction. A remarkable example of inversion was presented by Zheng and Hintelmann.[67] The efficiency of magnetic isotope selection produced by the singlet pair is lower than that produced by the triplet pair.[9] This prediction is also in excellent agreement with experimental observation: the extent of isotope separation was much lower in the dark reaction compared to photoreduction.[67]

A competition between singlet and triplet reaction channels was convincingly shown to depend on the nature of ligands bound to the Hg^{II} ion.[73] Photolysis of Hg^{II} with sulfurless ligands is a rather fast process resulting in positive MIE (enrichment of the reactant Hg^{II} phase in magnetic isotopes). Contrary to this, photolysis of Hg^{II} with sulfur-containing ligands occurs at low rates and results in negative MIE (depletion of magnetic isotopes in the reactant Hg^{II} and enrichment in the product Hg^0 phase). These observations clearly indicate that sulfurless ligands direct photolysis through the triplet channel, while sulfur-containing ligands stimulate the low-efficient singlet channel. This is important isotope signature elucidating chemical trans-

formation of mercury compounds. The authors [73] claim that even the NVE seems to be noticeable in the singlet channel at low magnitudes of the MIE.

As an example of dissociation reactions we will consider the dissociation of CH_3HgX, which is supposed to be the most important in production of Hg^0, the main pollutant.

Photoinduced dissociation occurs by generation of a triplet radical pair which directs magnetic nuclei into regenerated CH_3HgX (like in the case of photoreduction); nonmagnetic nuclei are predominantly accumulated in products. Photolysis of bis(*p*-trifluoromethylbenzyl)mercury (see above) exhibits just this mode of fractionation; the other brilliant experiment [61] on CH_3HgX photodegradation in the conditions close to natural ones exhibits the same mode, namely, the residual CH_3HgX was enriched in ^{199}Hg, ^{201}Hg ($\Delta^{201}Hg/\Delta^{199}Hg \approx 1.0-0.8$). In the dark reactions, fractionation proceeds in the opposite direction (Scheme 12).

Scheme 12

$$CH_3HgX \underset{^{199}Hg,\ ^{201}Hg}{\overset{h\nu}{\rightleftharpoons}} [CH_3^{\bullet}\ {}^{\bullet}HgX]^T \xrightarrow[^{200}Hg,\ ^{202}Hg]{} \text{products}$$

$$\Delta^{201}Hg/\Delta^{199}Hg = 1.05-1.25 \;||\; \Delta^{201}Hg/\Delta^{199}Hg = 0.80-0.95$$

$$CH_3HgX \underset{^{200}Hg,\ ^{202}Hg}{\overset{kT}{\rightleftharpoons}} [CH_3^{\bullet}\ {}^{\bullet}HgX]^S \xrightarrow[^{199}Hg,\ ^{201}Hg]{} \text{products}$$

$$\Delta^{201}Hg/\Delta^{199}Hg = 0.80-0.95 \;||\; \Delta^{201}Hg/\Delta^{199}Hg = 1.05-1.25$$

Note that atomic mercury may be formed by direct electron transfer to $HgCl^+$:

$$HgCl^+ + D \longrightarrow Hg^0 + D + (Cl^{\bullet}) \qquad (17)$$

Note that $HgCl^+$ is always present in water in equilibrium

$$HgCl_2 \rightleftharpoons HgCl^+ + Cl^- \qquad (18)$$

Schemes 11 and 12 allow one to identify the mechanisms both qualitatively (by the sign of fractionation) and quantitatively (by the numerical value of the ratio $\Delta^{201}Hg/\Delta^{199}Hg$). Inversion of the sign is an unambiguous qualitative diagnostic signature of the radical mechanism; the ratio $\Delta^{201}Hg/\Delta^{199}Hg$ is a physically reliable but quantitatively approximate parameter; even in terms of firmly established radical mechanism, the ratio $\Delta^{201}Hg/\Delta^{199}Hg$ may deviate from its canonical magnitudes $1.05-1.25$ (see Section 14 about the reasons).

12. Isotope fractionation in nonchemical processes

Since the energy of valence electrons depends on the nuclear volume, the ionization potentials and electron affinities are partly controlled by the nuclear volume; therefore, intermolecular, noncovalent bonds should also depend on it. For this reason, NVE is expected to manifest itself in such processes as evaporation, adsorption, extraction, bonding to ligands, ligand exchange, *etc*. In fact, it is in these nonchemical processes that NVE demonstrates itself most clearly.[70]

Extensive treatment of the NVE in crystals was reported by Schauble;[74] in particular, the NVE contributions to vapour – crystal mass-independent isotope fractionation calculated for elemental cadmium and mercury were in good agreement with experiments. Liquid – vapour mercury isotope fractionation was investigated under equilibrium and dynamic conditions by Estrade *et al.*;[75] mass-independent isotope fractionation in condensed mercury vapour with a $\Delta^{201}Hg/\Delta^{199}Hg$ ratio of about 0.83 was also detected; this value is very close to that expected for NVE-induced isotope selection.

The NVE is expected to be the most efficient in ligand exchange processes such as extraction, chromatography, *etc*.[49,76] A strontium isotope effect in the liquid – liquid extraction of strontium chloride by crown ether explained in terms of the NVE was found by Nishizava *et al.*[77] Anomalous isotope effect was found in isotope enrichment of ^{235}U in a redox reaction involving ligand exchange as the limiting step.[78,79]

The isotope enrichment factors for the even isotopes ^{234}U, ^{236}U and ^{238}U have shown a mass-dependent line, while that for ^{235}U deviated from the line; this evidences the NVE functioning, although the MIE contribution cannot also be excluded. Nomura *et al.*[80] found an ^{233}U isotopic anomaly in the $U^{4+} - U^{6+}$ exchange reaction; they noted that the isotope effect correlated with the isotope shifts of the lines in the atomic spectra of uranium isotopes. A review on the NVE was reported by Malinovsky *et al.*[81] with special emphasis on the analytical techniques. Note that Cai and Chen [82] were able to detect mass-independent fractionation even for the even isotopes ^{200}Hg and ^{202}Hg; only NVE is supposed to be responsible for this effect. Nevertheless, this result remains intriguing and needs to be reproduced.

13. Magnetic isotopes of mercury in living organisms

It is of paramount importance to elucidate isotope fractionation as a signature of reaction mechanisms inside living organisms, particularly, in the chemical transformation of methylmercury chloride (MMC), which is now considered as one of the most dangerous pollutants; MMC promotes a hardest neurological syndrome known as Minamata disease.[83] The first observation of the MIE-induced mercury isotope fractionation in the ATP enzymatic synthesis by creatine kinase (CK) was announced in 2004.[84]

In order to elucidate the mechanism of the MMC toxic effect, the authors have studied the CK enzymatic activity as a function of different isotopic forms of MMC, namely, $CH_3{}^{199}HgCl$, $CH_3{}^{200}HgCl$, $CH_3{}^{201}HgCl$ and $H_3C^{202}HgCl$. The relative activity of CK is plotted *vs*. MMC concentration in Fig. 12, which demonstrates remarkable features. First, a significant stimulation of CK activity is observed at low concentrations of $CH_3{}^{199}HgCl$ and $CH_3{}^{201}HgCl$, whereas there is no such effect for $CH_3{}^{200}HgCl$ and $CH_3{}^{202}HgCl$. Second, the suppression of the CK activity induced by high concentrations of MMC is very sensitive to the mercury isotopes (Fig. 12).

Thus, the loss of the half of the enzymatic activity occurs at a concentration of 42 mM for MMC with magnetic nuclei ^{199}Hg and ^{201}Hg (*cf*. 2.8 mM for MMC with nonmagnetic nuclei ^{200}Hg and ^{202}Hg). For MMC with a natural abundance of Hg isotopes, this concentration falls between these two limits in approximate proportion of magnetic and nonmagnetic isotopes in natural abundance.

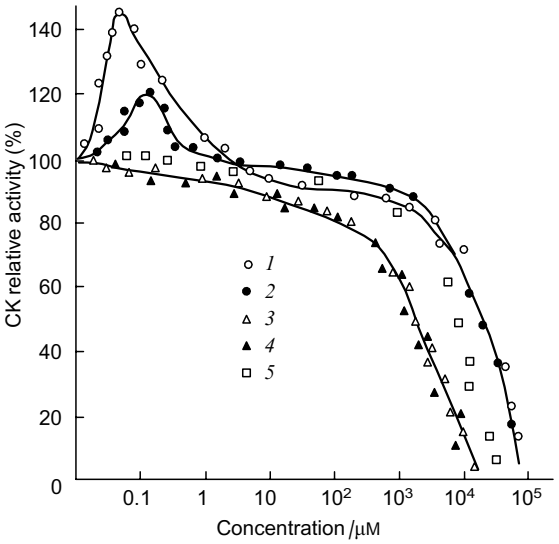


Figure 12. Creatine kinase activity as function of methylmercury chloride concentration for different isotopic forms of CH_3HgCl.[84] (*1*) ^{199}Hg, (*2*) ^{201}Hg, (*3*) ^{200}Hg, (*4*) ^{202}Hg, (*5*) Hg natural abundance.

The effect of mercury isotopes on the CK activity clearly indicates a reactivity difference between MMC molecules with magnetic and nonmagnetic nuclei. It is absolutely unbelievable that the difference in the nuclear mass would play any role in this effect. First, the mass differences are too small to cause any pronounced classical mass-dependent isotope effect; second, the experimentally measured effects are not selective to the masses of Hg nuclei but are highly sensitive to nuclear magnetism.

Nuclear spin selectivity of the reaction between CK and CH_3HgCl was confirmed by study of mercury isotope composition.[84] Some part of MMC molecules was shown to be chemically bound to CK. For the MMC with natural abundance of mercury isotopes, incubated with CK, the isotopic composition of CK with chemically bound MMC was measured. The results presented in Fig. 13 convincingly demonstrate isotope fractionation in the reaction of CK with MMC, namely, the MMC molecules grafted to CK are highly enriched in magnetic isotopes and depleted of nonmagnetic Hg nuclei.

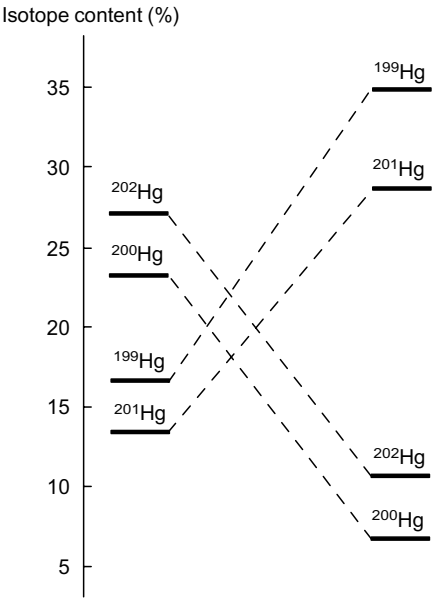


Figure 13. Mercury isotope contents in CH_3HgCl before incubation (on the left) with CK and in the CK with grafted CH_3HgCl (after incubation, on the right).[84]

Fractionation of magnetic and nonmagnetic isotopes reliably demonstrates that the interaction of CH_3HgCl with CK is a radical, nuclear spin-selective process. One of the key structural elements of the active site in CK is the cysteine residue (Cys), which keeps creatine anchored and positions it precisely along the enzyme reaction coordinate. This residue in the CK active site is the most vulnerable with respect to MMC. One can suppose that the interaction between CH_3HgCl and SH fragment of Cys (denote it as RSH) in the enzyme site is responsible for isotope fractionation in CK; the suggested mechanism of the reaction is shown in Scheme 13. The first step is the thermally induced generation of the singlet radical pair by electron transfer.

Scheme 13

$$CH_3HgCl + HSR \underset{^{200}Hg,\ ^{202}Hg}{\rightleftharpoons} |CH_3\dot{H}gCl^-\ {}^+H\dot{S}R|^S \xrightarrow[^{199}Hg,\ ^{201}Hg]{}$$

$$\longrightarrow |CH_3\dot{H}gCl^-\ {}^+H\dot{S}R|^T \xrightarrow[-HCl]{} |CH_3Hg^{\bullet}\ {}^{\bullet}SR| \longrightarrow$$

$$\longrightarrow CH_3HgSR$$

This pair can either regenerate the starting reactants by back electron transfer or undergo singlet–triplet spin conversion induced by the magnetic interaction of the unpaired electron in the $CH_3HgCl^{-\bullet}$ radical with magnetic nuclei ^{199}Hg and ^{201}Hg. Hyperfine coupling transforms singlet pairs with magnetic nuclei into triplet ones. Singlet–triplet conversion of the pairs with nonmagnetic isotopes (^{200}Hg, ^{202}Hg) is delayed and these pairs regenerate the starting reactants by back electron transfer. Finally, CK with grafted CH_3HgCl carries an excess of the magnetic nuclei ^{199}Hg and ^{201}Hg.[84]

This is the first example of the magnetic isotope effect operating in biochemical system. The effect manifests itself both in the nuclear spin-dependent enzyme activity and in isotope fractionation. The magnitude of the latter is rather large, being determined by favourable combination of the parameters characterizing the molecular, spin and chemical dynamics of the radical pair. It is a happy chance of combination of the dynamic parameters that were theoretically predicted[9] to result in highly efficient isotope sorting.

The addition of CH_3HgCl to SH fragment seems to be a universal chemical mechanism for mercury to enter living organisms *via* enzymatic reactions, because the great majority of enzymes contain SH groups in catalytic sites which are able to attach mercury species by addition reaction similarly to creatine kinase.

Extensive studies of mercury isotope fractionation were carried out recently[85–89] to elucidate how mercury is inherited and transferred along the trophic chains and what environmental factors, including industrial activity, control the metabolism and evolution of mercury as a

pollutant. Remarkable results were presented by Kwon *et al.*,[90] who detected no fractionation of mercury isotopes during trophic transfer of methylmercury.

Fractionation of stable isotopes of mercury during degradation of monomethylmercury to volatile elemental Hg and methane *via* the microbial Hg resistance pathway in *Escherichia coli*, carrying a mercury resistance genetic system, deserves special attention.[91] In the microbial monomethylmercury degradation, isotope fractionation was shown to depend on the cell densities: at lower density, enzyme catalysis functions, while at higher cell densities, the rate-limiting step is transport into the cell which does not cause isotope fractionation. The authors suggested that the MIE is also unlikely to occur during other microbial Hg transformations.[91] A recently published review of global environmental mercury processes in response to human perturbations and climate is also worthy of attention.[92]

14. Conclusion: achievements and problems

Fractionation of isotopes (particularly, of those with magnetic nuclei) is a powerful and often one and only tool for tracing the pathways and elucidating the mechanisms of geochemical reactions. However, it is necessary to deliberate that further progress in the use of magnetic isotopes meets some uncertainties and problems which should be kept in mind in order to prevent a danger of errors and speculations. Conclusions on the existence of mass-independent fractionation are not always worthy of confidence, particularly when the magnitudes of Δ do not much exceed the error limits. The magnitudes of Δ are usually determined in two ways. The first is to directly measure the deviations of the δ values for magnetic isotopes from those for nonmagnetic isotopes. Excellent examples are the Δ^{199}Hg values measured by Bergquist and Blum[61] (see Fig. 11) and by Zheng and Hintelmann,[67] which exhibit large differences in the fractionation of magnetic and nonmagnetic isotopes. The other way is to use regression equations similar to those employed to determine Δ values for mercury isotopes;[16] they were derived on the basis of the kinetic transition state theory and corrected as the difference between the measured δ values and those predicted by the mass-dependent effect. It is necessary to be aware that these regression equations are approximate, in particular, for small Δ values.

Yet another source of uncertainty is a superposition of different spin-selective reactions in processes with complicated mechanism. Each of these reactions may contribute to the total, experimentally measured, isotope fractionation with different magnitudes and signs of the effects, depending on the partners in radical pairs and their spin multiplicity. Finally, this results in scrambling of isotope distribution. Reversible reactions may be an additional source of isotope scrambling. In these cases, it seems to be useful to modify the reaction mechanism (for instance, by adding inhibitors or radical scavengers) and to detect changes in both fractionation sign and magnitude. The superposition and interference of different reactions is an important factor, which restricts and in fact puts a limit on the reliability of conclusions concerning the mechanisms of complicated, multistep reactions; it seems to be a bottleneck for unambiguous understanding of the isotope signatures.

The author is deeply thankful to Mark Thiemens for his inspiring and benevolent comments to the manuscript. Financial support from the Russian Science Foundation (Grant No. 14-23-00018) is also acknowledged.

References

1. R.G.Lawler, G.T.Evans. *Ind. Chim. Belges*, **36**, 1087 (1971)
2. A.L.Buchachenko, G.A.Nikiforov. *Dokl. Akad. Nauk USSR*, **228**, 379 (1976)
3. A.L.Buchachenko. *Russ. J. Phys. Chem.* **51**, 1445 (1977)
4. A.L.Buchachenko. *Chem. Rev.*, **95**, 2507 (1995)
5. A.L.Buchachenko. *J. Phys. Chem. A*, **105**, 9995 (2001)
6. A.L.Buchachenko. *Pure Appl. Chem.*, **72**, 2243 (2000)
7. A.L.Buchachenko. *J. Phys. Chem. B*, **117**, 2231 (2013)
8. A.L.Buchachenko, R.G.Lawler. *Acc. Chem. Res.*, **50**, 877 (2017)
9. A.L.Buchachenko. *Magnetic Isotope Effect in Chemistry and Biochemistry*. (New York: Nova Science Publishers, 2009)
10. A.L.Buchachenko. *Magneto-Biology and Medicine*. (New York: Nova Science Publishers, 2015)
11. J.Bigeleisen. *J. Am. Chem. Soc.*, **118**, 3676 (1996)
12. E.A.Schauble. *Geochim. Cosmochim. Acta*, **71**, 2170 (2007)
13. J.Bigeleisen. *Proc. Natl. Acad. Sci. USA*, **93**, 9393 (1996)
14. J.Bigeleisen. *Proc. Natl. Acad. Sci. USA*, **95**, 4808 (1998)
15. J.M.Eiler, B.Bergquist, I.Bourg, P.Cartigny, J.Farquhar, A.Gagnon, W.Guog, I.Halevy, A.Hofmann, T.E.Larson, N.Levin, E.A.Schauble, D.Stolper. *Chem. Geol.*, **372**, 119 (2014)
16. J.D.Blum, L.S.Sherman, M.W.Johnson. *Annu. Rev. Earth Planet. Sci.*, **42**, 249 (2014)
17. J.R.Hulston, H.G.Thode. *J. Geophys. Res.*, **70**, 3475 (1965)
18. R.N.Clayton, L.Grossman, T.K.Mayeda. *Science*, **182**, 485 (1973)
19. R.N.Clayton. *Ann. Rev. Earth Planet. Sci.*, **21**, 115 (1993)
20. M.H.Thiemens, J.E.Heidenreich III. *Science*, **219**, 1073 (1983)
21. M.H.Thiemens. *Annu. Rev. Earth Planet. Sci.*, **34**, 217 (2006)
22. M.H.Thiemens. *Proc. Nat. Acad. Sci.*, **110**, 17631 (2013)
23. R.E.Weston Jr. *Chem. Rev.*, **99**, 2115 (1999)
24. R.E.Weston Jr, in *Isotope Effects in Chemistry and Biology*. (Eds A.Kohen, H.-H.Limbach). (Boca Raton, FL: Taylor and Francis Group, 2006)
25. A.A.Wiegel, A.S.Cole, K.Hoag, E.L.Atlas, S.M.Schauffler. K.A.Boering. *Proc. Nat. Acad. Sci.*, **110**, 17680 (2013)
26. R.AMarcus. *J. Chem. Phys.*, **121**, 8201 (2004)
27. F.Robert. C.Camy-Peret. *Ann. Geophys.*, **19**, 229 (2001)
28. A.L.Buchachenko, A.V.Fedorov, L.LYasina. *Chem. Phys. Lett.*, **103**, 405 (1984)
29. L.L.Yasina, A.L.Buchachenko. *Chem. Phys.*, **146**, 225 (1990)
30. M.J.Raiti, M.D.Sevilla. *J. Phys. Chem. A*, **103**, 1619 (1999)
31. A.L.Buchachenko, L.L.Yasina, V.ABelyakov. *J. Phys. Chem.*, **99**, 4964 (1995)
32. A.LBuchachenko, E.O.Dubinina. *J. Phys. Chem. A*, **115**, 3196 (2011)
33. B.Luz, E.Barkan, M.L.Bender, M.H.Thiemens, K.A.Boering. *Nature (London)*, **400**, 547 (1999)
34. B.Luz, E.Barkan. *Science*, **288**, 2028 (2000)
35. B.Luz, E.Barkan, R.Yam, AShemesh. *Geochim. Cosmochim. Acta*, **73**, 6697 (2009)
36. T.A.Velivetskaya, A.V.Ignatiev, S.Y.Budnitskiy, V.V.Yakovenko, S.V.Vysotskiy. *Geochim. Cosmochim. Acta*, **193**, 54 (2016)
37. M.F.Miller, I.A.Franchi, M.H.Thiemens, T.L.Jackson. *Proc. Nat. Acad. Sci. USA*, **99**, 10988 (2002)
38. M.F.Miller. *Geochim. Cosmochim. Acta*, **66**, 1881 (2002)
39. M.F.Miller, A.LBuchachenko, E.Bailey, P.F.McMillan, M.H.Thiemens. *The Sixth International Symposium on Isotopomers. Program and Abstracts. Carnegie Institution of Washington, DC, 2012*. P. 37

40. E.N.Step, V.F.Tarasov, A.LBuchachenko. *Nature (London)*, **345**, 25 (1990)
41. E.N.Step, A.L.Buchachenko, N.J.Turro. *Chem. Phys.*, **162**, 189 (1992)
42. M.Wakasa, in *Dynamic Spin Chemistry*. (Eds S.Nagakura, H.Hayashi, T.Azumi). (Tokyo: Wiley, 1998)
43. H.Oduro, B.Harms, H.O.Sintim, A.J.Kaufman, G.Cody, J.Farquhar. *The Sixth International Symposium on Isotopomers. Program and Abstracts. Carnegie Institution of Washington, DC, 2012.* P. 57
44. Y.Watanabe, J.Farquhar, H.Ohmoto. *Science*, **324**, 370 (2009)
45. H.Oduro, B.Harms, H.O.Sintim, A.J.Kaufman, G.Cody, J.Farquhar. *Proc. Nat. Acad. Sci. USA*, **108**, 17635 (2011)
46. J.Labidi, J.Farquhar, C.M.Alexander, D.L.Eldridge, H.Oduro. *Geochim. Cosmochim. Acta*, **196**, 326 (2017)
47. M.Amor, V.Busigny, P.Louvat, A.Gélabert, P.Cartigny, M.Durand-Dubief, G.Ona-Nguema, E.Alphandéry, I.Chebbi, F.Guyot. *Science*, **352**, 705 (2016)
48. K.W.Mandernack, D.A.Bazylinski, W.C.Shanks 111, T.D.Bullen. *Science*, **285**, 1892 (1999)
49. T.Fujii, F.Moynier, F.Albarède. *Chem. Geol.*, **267**, 139 (2009)
50. C.M.Wawryk, J.DFoden. *Geochim. Cosmochim. Acta*, **150**, 285 (2015)
51. A.L.Buchachenko, V.A.Roznyatovsky, V.L.Ivanov, Yu.A.Ustynyuk. *Mendeleev Commun.*, **15**, 4 (2005)
52. A.L.Buchachenko, V.L.Ivanov, V.A.Roznyatovsky, Yu.A.Ustynyuk. *J. Phys. Chem. A*, **110**, 3857 (2006)
53. M.Wakasa, H.Hayashi, T.Kobayashi, T.Takada. *J. Phys. Chem.*, **97**, 13444 (1993)
54. M.Wakasa, H.Hayashi, K.Ohara, T.Takada. *J. Am. Chem. Soc.*, **120**, 3227 (1998)
55. E.N.Step, V.F.Tarasov, A.L.Buchachenko. *Chem. Phys. Lett.*, **144**, 523 (1988)
56. O.Koplak, R.B.Morgunov, A.L.Buchachenko. *Chem. Phys. Lett.*, **560**, 29 (2013)
57. A.L.Buchachenko, I.V.Khudyakov. *Acc. Chem. Res.*, **24**, 177 (1991)
58. Landolt-Börnstein. *Numerical Data and Functional Relationships in Science and Technology. New Series. Vol. 17. Magnetic Properties of Free Radicals*. (Ed. H.Fischer). (Berlin: Springer-Verlag, 1990)
59. A.L.Buchachenko, V.L.Ivanov, V.A.Roznyatovskii, A.K.Vorob'ev, Y.AUstynyuk. *Dokl. Phys. Chem. Akad. Nauk*, **413**, 50 (2007)
60. A.L.Buchachenko, V.L.Ivanov, V.A.Roznyatovskii, A.K.Vorob'ev, Y.AUstynyuk. *Dokl. Phys. Chem. Akad. Nauk*, **420**, 85 (2008)
61. B.A.Bergquist, J.D.Blum. *Science*, **318**, 417 (2007)
62. S.Huang, D.Yuan, H.Lin, L.Sun, S.Lin. *Appl. Geochem.*, **76**, 159 (2017)
63. R.S.Smith, J.G.Wiederhold, A.D.Jew, G.E.Brown Jr., B.Bourdon, R.Kretzschmar. *Geochim. Cosmochim. Acta*, **137**, 1 (2014)
64. Q.Huang, J.Chen, W.Huang. *Atmos. Chem. Phys.*, **16**, 11773 (2016)
65. L.S.Sherman, J.D.Blum, D.K.Nordstrom, R.B.McCleskey, T.Barkay, C.Vetriani. *Earth and Planetary Sci. Lett.*, **279**, 86 (2009)
66. E.Sunderland, C.Driscoll, J.Hammitt, P.Grandjean, J.Evans, J.D.Blum, C.Chen, D.Evers, D.Jaffe, R.Mason, S.Goho, W.Jacobs. *Environ. Sci. Tech. Lett.*, **50**, 2117 (2016)
67. W.Zheng, H.Hintelmann. *Geochim. Cosmochim. Acta*, **73**, 6704 (2009)
68. M.Jimenez-Moreno, J.P.G.Barre, V.Perrot, S.Berail, R.C.Rodríguez Martín-Doimeadios, D.Amouroux. *Chemosphere*, **147**, 430 (2016)
69. L.Zhang, Y.Liu, L.Guo, D.Yang, Z.Fang, T.Chen, H.Ren, B.Yu. *Tectonophysics*, **79**, 619 (2014)
70. A.L.Buchachenko. *Russ. Chem. Rev.*, **78**, 319 (2009)
71. J.E.Sonke. *Geochim. Cosmochim. Acta*, **75**, 4577 (2011)
72. S.Ghosh, Y.Xu, M.Humayun, L.Odom. *Geochem. Geophys. Geosystems*, **9**, 1 (2008)
73. W.Zheng, H.Hintelmann. *J. Phys. Chem. A*, **114**, 4246 (2010)
74. E.A.Schauble. *Proc. Nat. Acad. Sci. USA*, **110**, 17714 (2013)
75. N.Estrade, J.Carignan, J.E.Sonke, O.F.X.Donard. *Geochim. Cosmochim. Acta*, **73**, 2693 (2009)
76. F.Moynier, T.Fujii, P.Telouk. *Analyt. Chim. Acta*, **632**, 234 (2009)
77. M.Nishizawa, T.Satoyama, T.Miki, T.Yamamoto. *J. Nucl. Sci. Technol.*, **32**, 1230 (1995)
78. Y.Fujii, M.Nomura, M.Okamoto, H.Onitsuka, F.Kawakami, K.Takeda. *Z. Naturforsch. A,* **44**, 395 (1989)
79. Y.Fujii, M.Nomura, H.Onitsuka, K.Takeda. *J. Nucl. Sci. Technol.* **26**, 1061 (1989)
80. M.Nomura, N.Higuchi, Y.Fujii. *J. Am. Chem. Soc.*, **118**, 9127 (1996)
81. D.Malinovsky, F.Vanhaecke. *Anal. Bioanal. Chem.*, **400**, 1619 (2011)
82. H.Cai, J.Chen. *Sci. Bull.*, **61**, 116 (2016)
83. D.A.Kouznetsov, V.Richter. *Int. J. Neurosci.*, **34**, 1 (1987)
84. A.L.Buchachenko, D.A.Kouznetsov, A.V.Shishkov. *J. Phys. Chem. A*, **108**, 707 (2004)
85. K.Kritee, L.C.Motta, J.D.Blum, M.Tsui, J.R.Reinfelder. *ACS Earth Space Chem.*, 2 (5), 432 (2018)
86. R.A.Miserendino, J.R.D.Guimarães, G.Schudel, S.Ghosh, J.M.Godoy, E.K.Silbergeld, P.S.J.Lees, B.ABergquist. *ACS Earth Space Chem.*, 2 (5), 441 (2018)
87. T.A.Jackson. *Appl. Geochem.*, **71**, 86 (2016)
88. T.AJackson. *Geomicrobiology J.*, **32**, 799 (2015)
89. S.Y.Kwon, J.D.Blum, K.J.Nadelhoffer, J.T.Dvonch, M.T.Tsui. *Sci. Total Environ.*, **532**, 220 (2015)
90. S.Y.Kwon, J.D.Blum, M.J.Carvan, N.Basu, J.A.Head. *Environ. Sci. Technol.*, **46**, 7527 (2012)
91. K.Kritee, T.Barkay, J.D.Blum. *Geochim. Cosmochim. Acta*, **73**, 1285 (2009)
92. D.Obrist, J.L.Kirk, L.Zhang, E.M.Sunderland, M.Jiskra, N.E.Selin. *Ambio. J. Human Environ.*, **47**, 116 (2018); doi: 10.1007/s13280-017-1004-9